A novel wave breaking framework to estimate air-sea gas transfer velocities

Sophia E. Brumer[1,a], **Christopher J. Zappa**[1]

[1]Lamont-Doherty Earth Observatory of Columbia University, Palisades, NY, USA.

[a]Now at Laboratoire d'Océanographie Physique et Spatiale, UMR 6523 CNRS-IFREMER-IRD-UBO, IUEM, Plouzané, France

Key Points:

- a novel gas transfer velocity parameterization is proposed for wave breaking conditions
- modeling turbulence- and bubble-mediated gas transfer using breaking crest length distribution
- tested using breaking crest length distribution and gas flux measurements from HiWinGS

Corresponding author: Sophia E. Brumer, `sophia.brumer@ifremer.fr`

Abstract

Parameterizations of gas transfer velocities are needed for climate predictions. Single parameter models typically only include wind dependence and may readily be used in climate studies. Their application is however gas specific and limited to select environments. Mechanistic parameterizations incorporating multiple forcing factors allow modelling the transfer of gases with differing solubilities for a wide range of conditions. A novel framework is put forward to model gas transfer in the open ocean in the presence of breaking waves. It incorporates both the turbulence- and bubble-mediated transfers based on statistics determined from the breaking crest length distribution ($\Lambda(c)$). Testing the mechanistic model with measurements from the HiWinGS field campaign shows promising results for both CO_2 and DMS. Uncertainties remain in the quantification of bubble clouds which are at the core of the formulation of the bubble-mediated transfer.

Plain Language Summary

Predicting climate change relies on models of the transfer of gases across the atmosphere-ocean interface. Traditionally for every gas a different function of wind speed is used to compute its transfer velocity and air-sea flux. These functions are valid only in specific environmental conditions. To improve predictions, models that account for the different transfer mechanisms have to be developed. Ideally they are applicable to any gases regardless of solubility. Such a model is put forward herein. It allows to estimate the transfer velocities based on remote sensing of breaking waves and the wave field accounting for both the transfer due to turbulence and bubbles. The model is tested with measurements from the HiWinGS field campaign and shows promising results for both CO_2 and DMS. Remaining uncertainties and limitations are discussed highlighting the need for open ocean measurements of breaking waves and their associated bubble plume.

1 Introduction

Modelling air-sea gas fluxes is essential for climate predictions and relies on estimates of the gas transfer velocity (k) which is typically parameterized as a function of the 10-m wind speed (e.g. Wanninkhof, 1992; Ho et al., 2011). Large scatter is observed in estimated gas transfer velocities (k) of sparingly soluble gases at high wind speeds where wave breaking dominates upper ocean dynamics (Blomquist et al., 2017; Brumer et al., 2017a). The removal of this scatter by a wind-wave based parameterization (Brumer et al.,

2017a) suggests that k would be better modeled with the inclusion of surface wave breaking rather than wind speed alone.

Wave breaking has the potential to considerably impact air-sea exchanges and upper-ocean dynamics (Deike, 2022). It leads to enhanced turbulent kinetic energy (TKE) in the near surface layer resulting in surface TKE dissipation rates (ε) shown to be roughly 5 to 1000 times greater than predicted by wall layer scaling (Agrawal et al., 1992; Gemmrich, 2010; Sutherland and Melville, 2015; Terray et al., 1996). Additionally, air-entraining breaking waves generate bubble clouds that allow for an additional pathway for gas transfer which is particularly important to consider for sparingly soluble gases such as CO_2 (Woolf, 1993).

Efforts have been made to account for the impact of bubbles in physical process based models (Deike and Melville, 2018; Fairall et al., 2011; Liang et al., 2013; Goddijn-Murphy et al., 2016; Asher et al., 1996). Only one of these models explicitly considers the contribution of wave breaking turbulence (Asher et al., 1996; Asher and Wanninkhof, 1998). However, it is reduced to a function of the whitecap cover and 10-m wind speed. None of these models include direct dependence of the transfer to the TKE dissipation due to wave breaking, it is implicitly comprised through dependence on the friction velocity amongst other forcing. While all these variables are inter-linked, it is not always in a straight forward way. The limitations of these models were revealed using the whitecap coverage and the gas transfer velocities of CO_2 and DMS observed during HiWinGS (Blomquist et al., 2017).

Several studies have shown how enhanced turbulence promotes gas transfer (Zappa et al., 2007; Tokoro et al., 2008; Vachon et al., 2010; Esters et al., 2017) but not in relation to breaking waves. Based on measurements of turbulence in the wave-affected and wave breaking layers, Shuiqing and Dongliang (2016) derived a parameterization for the gas transfer velocity in the presence of breaking waves. Their proposed functional form is similar to that of Asher and Wanninkhof (1998) without the bubble-mediated component. It does not directly depend on the turbulent kinetic energy dissipation rate, but rather the air friction velocity, the whitecap cover, and wave age.

Herein, a novel framework to model air-sea gas transfer velocities in the presence of breaking waves is put forth. The proposed framework incorporates both the turbulence- and bubble-mediated transfer. It is based on two statistics derived from the breaking crest

length distribution (Phillips, 1985): the turbulent kinetic energy dissipation rate and the bubble volume flux. Multiple field campaigns in the last decade have demonstrated the existence of a robust link between the breaking crest length distribution to the turbulent kinetic energy dissipation rate following the spectral framework proposed by Phillips (1985) to quantify wave breaking properties. Recently, through a combination of DNS and laboratory observations Deike et al. (2017) have extended the application of the Phillips (1985) framework allowing estimations of bubble cloud properties from the breaking crest length distribution. These advances are at the core of the present framework.

Section 2 provides an outline of the general form of the proposed model followed by a review of Phillips (1985)'s theoretical framework and the work of Deike et al. (2017) which are used for the derivation of quantities key to air-sea gas transfer. The model is tuned using data from the High Wind Gas Exchange Study (HiWinGS) which is shown in section 3. The model is compared to other existing physically-based models in sections 4 where uncertainties and guidelines for future measurements are also discussed.

2 Proposed Gas Transfer Model

The proposed functional form of the k model accounting for the contribution of the turbulence-driven (k_ε) and the bubble-mediated (k_b) transfers is:

$$k = k_\varepsilon + k_b \tag{1}$$

Various mechanistic approaches were suggested by which turbulence promotes the transfer of gases. These invoke concepts of surface renewal (Higbie, 1935; Danckwerts, 1951; Lamont and Scott, 1970; Komori et al., 1993), surface penetration (Harriott, 1962; Atmane et al., 2004) and surface divergence (McCready et al., 1986; Banerjee and MacIntyre, 2004; Banerjee et al., 2004; McKenna and McGillis, 2004; Turney et al., 2005) and their application is limited to a constrained set of environmental conditions. Boundary layer scaling arguments also allow to derive k_ε. The flux of gas (F_g) follows Fick's law of diffusion:

$$F_g = D\frac{\partial C}{\partial z} = \frac{D}{\delta_z}(C_w - \alpha C_a) = k_\varepsilon(C_w - \alpha C_a) \tag{2}$$

Where D is the diffusivity, δ_Z a characteristic surface boundary length scale, α the Ostwald solubility coefficient and C_a, C_w the air and water concentrations, respectively. This allows rewriting k_ε as:

$$k_\varepsilon = \frac{D}{\delta_z} \tag{3}$$

Using the Batchelor length scale $\delta_Z \propto \left(\frac{\nu_w D^2}{\varepsilon}\right)^{\frac{1}{4}}$, which is the characteristic turbulent microscale for a passive scalar (Batchelor, 1959), the following relationship between k_ε and ε was derived (Banerjee et al., 1968; Kitaigorodskii, 1984):

$$k_\varepsilon \propto (\varepsilon \nu_w)^{\frac{1}{4}} Sc^{-0.5} \tag{4}$$

where ν_w is the water viscosity, and $Sc(=\nu_w/D)$ is the water-side Schmidt number defined as the ratio of the water viscosity and the mass diffusivity D .

The bubble-mediated transfer is commonly expressed as function of the bubble volume flux (F_a) or the void fraction (v) (Woolf, 1997; Woolf et al., 2007). Neglecting potential collective effects of bubbles Woolf proposed the so-called "independent bubble model":

$$k_{b_{ind}} \propto F_a \alpha^{-1} \left(1 + (\chi)^{1/1.2}\right)^{-1.2} \tag{5}$$

with

$$\chi \propto Sc^{-0.5} F_a \alpha^{-1} \tag{6}$$

It satisfies the two commonly accepted distinct asymptotic behaviours of k_b: 1) for highly soluble gases ($\alpha >> 1$), where full equilibration is achieved, the bubble-mediated flux is limited by the bubble volume flux and solubility and 2) for very weakly soluble gases ($\alpha << 1$), where no equilibration is achieved, the flux does not depend on solubility but on diffusion (see also Keeling (1993); Goddijn-Murphy et al. (2016); **?**).

Based on laboratory work by Cipriano and Blanchard (1981), Woolf (1997) first suggests that:

$$F_a = 6.25 \times W \text{ [m(m}^2 \text{ s)}^{-1}\text{]} = 2250 \times W \text{ [cm hr}^{-1}\text{]} \tag{7}$$

and

$$\chi = \frac{Sc^{-0.5}}{14\alpha} \tag{8}$$

Where W is the total whitecap cover expressed as a fraction. Later in the paper, Woolf uses $F_a = 2450W$ which is the value adopted by subsequent studies. Note that Eq. (8) removes the additional higher order F_a dependence of Eq. (5).

2.1 Phillips' [1985] Spectral Framework

Laboratory experiments by Duncan (1981, 1983), in which a breaking wave was created by a hydrophoil towed at constant speed and depth, revealed a relationship between

energy dissipated by a steady breaking wave and its speed:

$$\varepsilon_l \propto \frac{\rho_w c_h^5}{g}, \tag{9}$$

where ε_l is the energy dissipation per crest length, ρ_w is the water density, g is the gravitational acceleration, and c_h the speed of a towed hydrofoil which corresponds to the speed of the breaking crest, $c_h \sim c_{br}$.

Phillips (1985) introduced the spectral density of the breaking crest length per unit area $\Lambda(c)$, where c is the breaking wave phase speed. Based on Duncan's experiments, he proposed:

$$\varepsilon = \int S_{ds}(c)dc = \int b(c)\rho_w g^{-1} c^5 \Lambda(c)dc \tag{10}$$

where S_{ds} is the spectral dissipation term from the radiative transfer equation that describes the evolution of the wave field and $b(c)$ is the spectral breaking strength.

Recognizing the value of the breaking crest length distribution to infer breaking wave characteristics and subsequently air-sea interaction processes, multiple studies have been undertaken to obtain direct measurements of both $\Lambda(c)$ and ε. The first measurements of $\Lambda(c)$ were made by Phillips et al. (2001) using a marine radar. Later studies have used digital video camera to track breaking waves from stable platforms (Gemmrich et al., 2008, 2013; Schwendeman et al., 2014; Sutherland and Melville, 2013, 2015; Thomson et al., 2009; Zappa et al., 2012) and planes (Kleiss and Melville, 2010). Techniques to derive the breaking crest length distribution from the imagery vary greatly. These are reviewed and discussed in Banner et al. (2014). Here, the initial velocity method is adopted, in which the phase velocity c is equated to a fixed reference velocity that corresponds to initial breaker-front velocity of each breaking event (c_{br}) as was originally chosen by Phillips (1985). The phase speed of the breaking wave has been shown to be closely related to the speed of the breaking crest c_{br} with $c_{br}/c \sim 0.8-0.9$. Following Gemmrich et al. (2008, 2013), the breaking crest length distribution $\Lambda(c_{br})$ for a given speed range (c_{br}, $c_{br} + \Delta c_{br}$) is then obtained from:

$$\Lambda(c_{br}) = \sum L_{br} t_{br} / (T A \Delta c_{br}) \tag{11}$$

where L_{br} is the characteristic breaking segment length, t_{br} duration of an individual breaking crest event (based on the time a breaker is tracked in the imagery), A is the area of the field of view, and T the total duration of observation.

2.2 Estimating the turbulent kinetic energy dissipation rate

To estimate the turbulent kinetic energy dissipation rate from the breaking crest length distribution (Eq. 10), one unknown remains: the spectral breaking strength $b(c)$. Wave systems produced in laboratory experiments are narrow-banded and $b(c)$ is assumed to be independent of scale. It was found to vary with wave steepness (Banner and Peirson, 2007; Drazen et al., 2008; Melville, 1994). Ocean waves are however rarely narrow-banded and modeling studies suggest that $b(c)$ may scale with wave age (**?**Romero et al., 2012).

No direct field measurements of b(c) exist to date as $\varepsilon(c)$ has not been tractable in the open ocean. A scale-independent effective breaking strength coefficient (b_{eff}) was thus defined:

$$b_{eff} = \frac{\varepsilon}{\rho_w g^{-1} \int c^5 \Lambda(c) dc} \tag{12}$$

Leading to:

$$\varepsilon(c) = b_{eff} c^5 \Lambda(c)/g \tag{13}$$

Reviewing all existing breaking crest length distribution and coinciding upper ocean dissipation rate measurements, Zappa et al. (2016) determined the following wave-age dependent parameterisation of b_{eff}:

$$b_{eff} = 3.48 \times 10^{-3} - 4.69 \times 10^{-5} \frac{c_p}{u_*} \tag{14}$$

Here c_p is the phase speed of the dominant wave and u_* the air friction velocity.

2.3 Estimating the Bubble Volume flux

Estimation of the bubble volume flux and void fractions are based on relations determined from novel direct numerical simulations (DNS) of three-dimensional breaking waves that resolve bubble scales (Deike et al., 2016). One of the key finding from this DNS study is that total volume of air entrained by a breaking wave (V_a) is directly proportional to the breaking crest length (L_{br}) and the breaking speed to the power 5:

$$V_a = B b_{eff} \frac{L_{br} c_{br}^5}{U_b g^2} \tag{15}$$

Where B is a dimensionless constant, and U_b is a dissipation-weighted vertical mean velocity which corresponds to the average rise velocity of the bubble plume. This relation stems from the core assumption that the global (integrated breaking event's spatio-temporal

extent) work done against buoyancy forces in entraining the bubbles is proportional to the mechanical energy dissipated where $B = 0.1$ is the proportionality factor. U_b scales as the rise velocity in clean water (Woolf and Thorpe, 1991) of a bubble of radius equal to the mean of the bubble distribution. Not knowing the bubble distribution, a constant U_b equal to 10 cm s^{-1} is assumed here based on Asher et al. (1997).

From Eq. 15, a volume flux per unit area (F_a) can be estimated by summing the total volume of air entrained by each breaker observed during a single video recording and dividing by the area of the field of view (A) and the total time of observations (T).

$$F_a = \frac{\sum V_a}{AT} = b_{eff} B \frac{\sum L_{br} c_{br}^5}{AT U_b g^2} \tag{16}$$

Alternatively, F_a may be expressed as a combination of the fifth moment of the breaking crest length distribution and the breaking duration (τ_{br}):

$$F_a = \frac{b_{eff} B}{U_b g^2} \int \frac{1}{\tau_{br}(c)} \Lambda(c) c^5 dc \tag{17}$$

This form assumes that the duration of the breaker is a function of the breaker speed. As proposed by Kleiss (2009), based on laboratory and field data (Thorpe and Hall, 1983; Rapp and Melville, 1990), τ_{br} can be related to the period of the breaking wave which may be expressed in terms of the phase speed c via the deep water dispersion relation:

$$\tau_{br} \propto \frac{2\pi}{g} c \tag{18}$$

Kleiss (2009) suggests $\tau_{br} = 0.25 c_{br}$, thus:

$$F_a = 4 \frac{b_{eff} B}{U_b g^2} \int \Lambda(c) c^4 dc \tag{19}$$

2.4 Calibrating the Model Framework

As it is the case for all existing gas transfer model, several proportionality constants remain to be determined. This can be done by solving:

$$k_\Lambda = \mathcal{A} K_\varepsilon + \mathcal{B} K_b \tag{20}$$

Where K_ε is equal to the right hand side of the relations in Eq. (4) and

$$K_b = F_a \alpha^{-1} \left(1 + \left(\mathcal{C} Sc^{-0.5} F_a \alpha^{-1}\right)^{1/1.2}\right)^{-1.2} \tag{21}$$

The coefficients $\mathcal{A}$, $\mathcal{B}$, and $\mathcal{C}$ should be obtained through least squared error regression using measurements derived transfer velocities of gases of varying solubilities over a wide range of wind and wave conditions.

3 HiWinGS application

The proposed framework was tuned using the gas transfer velocities of CO_2 and DMS derived from the eddy co-variance measurements taken during the 2013 HiWinGS field campaign. Details about HiWinGS can be found in (Blomquist et al., 2017; Brumer et al., 2017a,b; Yang et al., 2014). Breaking waves were monitored through high frequency video recording of 20 minutes in the visible band throughout the daytime. Momentum, heat, and gas fluxes were computed hourly. Figure 1 illustrates the variable space sampled during the experiment where concurrent good quality data is available. Hourly averaged 10-m neutral wind speed (U_{10N}) range from 8.3 to 25.1 m s^{-1}, the significant wave height (H_s) from 2.2 to 8.5 m for wave ages (c_p/u_*) of 12.2 to 51.7. The sea surface (SST) and air (T_a) temperatures ranged 6.3-20.6 and 2.7-12.5°C, respectively with differences, $\Delta T = T_a - \text{SST}$ spanning -10.9 to 1.8°C.

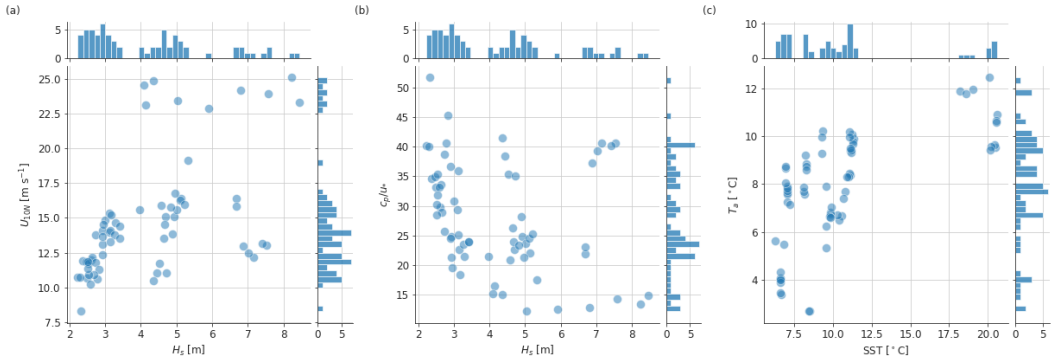

Figure 1. Scatter plots and histograms of (a) the neutral 10-m wind speed (U_{10N}) vs. the significant wave height (H_s), (b) the wave age (c_p/u_*) vs. the significant wave height, and (c) the surface air temperature (T_a) vs. the sea surface temperature (SST)

3.1 Tracking breaking crests

The breaking crest length distributions were determined from over 200 videos taken the starboard side of the flying bridge of the R/V Knorr. For details on the setup see Brumer et al. (2017b). All background gradients present in the images were removed prior to any further analysis. The images were then corrected for lens distortion and re-projected using the roll, pitch, and yaw angles measured by IMUs. Finally, they were interpolated

onto a regular grid with pixel resolution of 0.1 m. The area of the field of view A was ~ 1100 m^2 and the total duration of observation T was around 19 minutes.

The breaking crest lengths were tracked following the method developed by Gemmrich et al. (2008). In order to bring out the advancing side of the whitecap two consecutive rectified and projected images are differenced. As whitecaps are brighter than the background, the advancing front is distinguishable by high positive values, while the rear side is negative in the differenced image. The differenced images are thresholded based on image intensity (I) using $I/\max(I) > 0.6$ and transformed into binary images where the breaking crests have pixels equal to 1 and the rest is set to 0.

Using Matlab's image processing toolbox, a series of morphological operations are then applied to the binary frames to insure that crest do not contain holes and to link crests that are close together into a single one (details in Supplementary Information (SI)). Finally, each crest is identified and approximated as an ellipse. This allows to determine the coordinates of the center of mass of each crest, as well as the length major and minor axis, their area, and orientation.

At this stage crests that have an area smaller than 1.5 m^2 are removed. The remaining crests are then tracked from one differenced frame to the next. Matching the crests in consecutive differenced frames is based on:

1. propagation direction of the centers of mass of $\pm$ 90° relative to the ship's orientation which was pointed into the wind.
2. a propagation speed less than 1.2 times the phase speed of the waves at spectral peak.
3. change in area and major axis length less than 25%
4. orientations of the major axes within 15°

The theoretical minimum detectable crest advancement speed is dictated by the pixel resolution and the frame rate. A breaking crest can be seen to move from one frame to the next only if it traveled at least the equivalent distance of 1 pixel (0.1 m) in between acquisition (1/20 s). Thus, at the native frame rate only waves traveling at a minimum speed of 2 m s^{-1} are detectable. To reduce the resolvable propagation speed to 1 m s^{-1}, breaking waves were tracked in every other image. Note, however, that the coor-

dinates of the center of masses are determined within fractions of pixels thus propagation speeds smaller than 1 m s^{-1} can result from the analysis.

3.2 Breaking crest length distributions

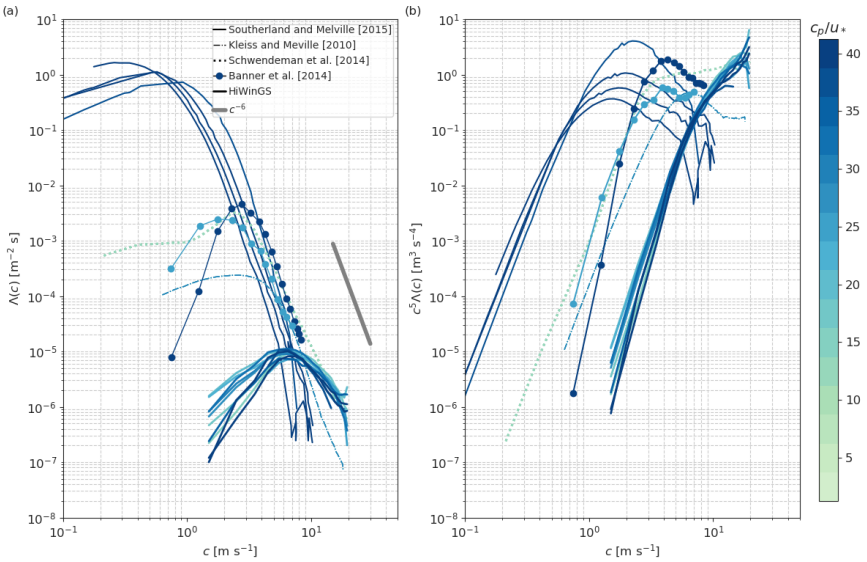

Figure 2. (a) Breaking crest length distributions and (b) their fifth moment as a function of the breaking crest speed color-coded by wave age ($\frac{c_p}{u_*}$).

Figure 2a shows the breaking crest length distributions as a function of the breaking speed computed from the HiWinGS data set color-coded by wave age ($\frac{c_p}{u_*}$). Figure 2b shows their fifth moment. Also shown are some of the previous breaking crest length determined from visible imagery. Much younger seas and higher winds were sampled during HiWinGS than during most of the previous field experiments outlined above. It is also important to note that different analysis techniques were used by the different groups. Only the two RaDyO datasets presented in Gemmrich et al. (2013) were analyzed with the technique used here. Mean breaking crest length distributions from Gemmrich's analysis are reported in Banner et al. (2014) and shown in 2. The discrepancies arising from the various analysis techniques and choices in independent variables (in particular c_{br}) used to compute the breaking crest length distributions were highlighted by Banner et al. (2014) and will not be discussed further here. Nevertheless, these systematic differences

have to be taken into consideration when comparing the breaking crest length distributions plotted here. The breaking crest length distribution computed from the HiWinGS data follow less closely the theoretical c^{-6} high c_{br} tail than previously published ones. This means that scalings for Λ such as those proposed by Sutherland and Melville (2013) or Deike and Melville (2018) poorly reproduce them (c.f. SI). There is no clear explanation for this discrepancy at this time.

3.3 Determining the Framework's Coefficients

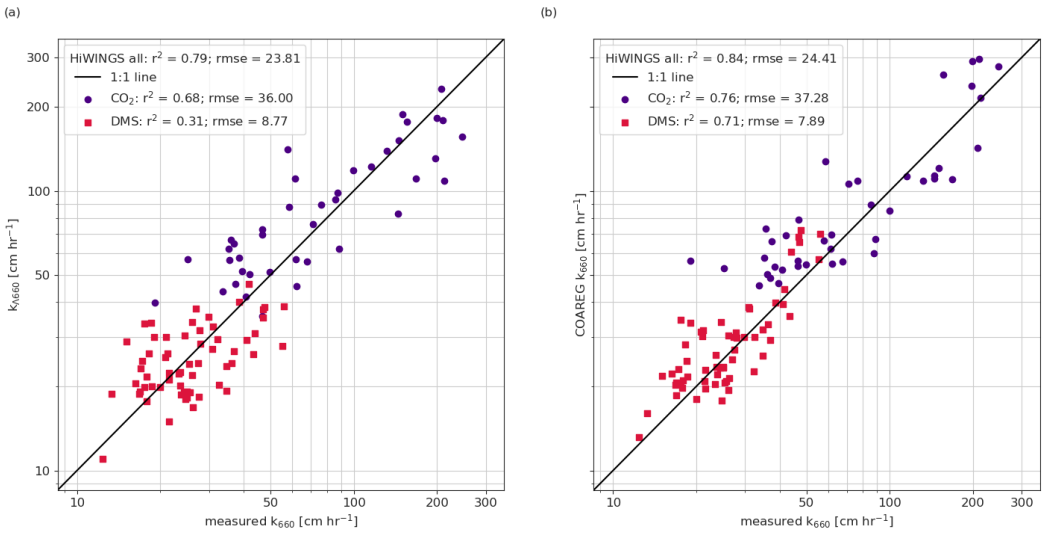

Figure 3. Scatter plots of (a) the k_Λ model proposed in Eq. 20: $k_{\Lambda 600} = 0.21K_\varepsilon + 3.26F_a\alpha^{-1}\left(1+\left(0.088Sc^{-0.5}F_a\alpha^{-1}\right)^{1/1.2}\right)^{-1.2}$ and (b) the COAREG model (see SI for equations) versus the gas transfer velocities of CO_2 (purple) and DMS (ruby) estimated from HiWinGS eddy-covariance flux measurements referenced to a Schmidt number of 660.

A non-linear least squares fit of the HiWinGS data within the proposed breaking framework for the gas transfer velocity k_Λ (Eq. 20) provides $\mathcal{A} = 0.211 \pm 0.034$, $\mathcal{B} = 3.26 \pm 0.574$, and $\mathcal{C} = 0.088 \pm 0.072$. Variability linked to the b_{eff} parameterization (Eq. 13) was propagated. Results are shown in Figure 3a. k_Λ from Equation 20 is able explain 79% of the overall variability in the measurement derived gas transfer velocities. The correlations to the transfer velocities of CO_2 ($r^2 = 0.68$) and DMS ($r^2 = 0.31$) individually are lower than for the overall fit, particularly for DMS. Output of NOAA's

COAREG algorithm (Blomquist et al. (2017); Fairall et al. (2011); equations in SI) for matching measurements are shown in Figure 3b allowing to evaluate the relative performance of the mechanistic model proposed by Eq. 20. COAREG is able to reproduce 76% and 71% of the transfer velocities of CO_2 and DMS, respectively. The root mean square errors of the two models are overall of the same order of magnitude: 23.81 cm hr^{-1} for the breaking crest length based model and 24.41 cm hr^{-1} for COAREG for CO_2 and DMS combined. Note that fixing $\mathcal{A}$ using the DMS data assuming no bubble contribution to its transfer ($k = \mathcal{A}K_\varepsilon$) and subsequently determining the other coefficients with the CO_2 data results in poorer fit statistics for DMS while not improving those for CO_2.

4 Discussion

4.1 Comparison to other mechanistic models

The base functional form of the model for k (Eq. 1) is a linear combination of parameterizations of transfer velocities arising from different processes. As such, it follows the form adopted by previous studies (Deike and Melville, 2018; Fairall et al., 2011; Asher and Wanninkhof, 1998). Unlike in COAREG, it does not take into account the air-side transfer and is therefore only applicable to sparingly and less soluble gases. This could explain its poorer performance, particularly for DMS.

No distinction is made between the turbulence-mediated transfer due to wave breaking and other processes as is done in Asher and Wanninkhof (1998); Shuiqing and Dongliang (2016). This is because computing the dissipation using the effective breaking strength gives an integrated estimate of the turbulence in the upper ocean at the given whitecap coverage and wave age. Indeed, b_{eff} was determined from the combination of breaking crest length distribution estimates and measures of the upper ocean turbulence that include both the wave breaking turbulence and the background turbulence (Zappa et al., 2016).

The proportionality coefficient $\mathcal{A} = 0.211 \pm 0.034$ that multiplies K_ε to give k_ε is within the range of those determined in previous studies none of which account for bubbles ($k = k_\varepsilon$). Zappa et al. (2007) suggested $\mathcal{A} = 0.4$ based on data collected in a large tidal river, a macro-tidal estuary, and from a coastal ocean site as well as in a "model" saltwater ocean at Biosphere 2 (Oracle, AZ USA) . Later studies by Tokoro et al. (2008) suggest $\mathcal{A} = 0.17$-0.18 for riverine and coastal environments while Vachon et al. (2010)

311 determined $\mathcal{A} = 0.39$-0.44 in freshwater systems. The first open ocean verification of the
312 functional form of k_ε suggest $\mathcal{A} = 0.12$-1.46 depending on the depth at which the tur-
313 bulent kinetic dissipation rate measurements were taken and the approach used to ex-
314 trapolate these measurements to the surface (Esters et al., 2017). Note that in this study
315 different values of $\mathcal{A}$ were determined for CO_2 and DMS as the transfer velocities of these
316 gases cannot be reconciled without taking bubble-mediated transfer into account. While
317 fitting the transfer velocities separately may have led to improved fit statistics, it would
318 defeat the goal of finding an unified model for both if not all gases. Since $\mathcal{A}$ depends on
319 the measurement of ε at the surface and observations vary greatly over the depth that
320 it is evaluated, direct comparison between studies is difficult. As shown in Zappa et al.
321 (2009), the near-surface dissipation can vary several orders of magnitude in the top 50
322 cm and will have a distinct impact on the gas transfer velocity. The value reported here
323 is one corresponding to an integrated dissipation over the depth of the wave boundary
324 layer roughly equal to the height of the wind-sea.

325 The form of the bubble-mediated transfer used in Asher and Wanninkhof (1998)
326 could not be used for this study because 1) a wider variety of solubility have to be con-
327 sidered to estimate the coefficients and there are more unknowns than gases available,
328 and 2) it accounts for wave breaking only via W. Asher and Wanninkhof (1998) devel-
329 oped their model using laboratory W which may have led to unrealistic estimates of both
330 the bubble and the wave breaking turbulence mediate transfers. One could easily use the
331 functional form proposed by Merlivat et al. (1993) for the bubble-mediated transfer with
332 the coefficients determined by Asher and Wanninkhof (1998) to estimate K_b in Eq. 20.
333 This however defeats the goal of a purely breaking crest length and sea state dependent
334 model.

335 Both Woolf (1997), Woolf et al. (2007) and Goddijn-Murphy et al. (2016) assumed
336 that the left and right hand side terms of Eq. 5 are equal rather than proportional. In
337 both the model proposed herein and COAREG k_b scaling is adjusted through the em-
338 pirical parameters $\mathcal{B}$ and $\mathcal{B}_{COAREG}$, respectively. Note that these cannot be set inde-
339 pendently from the models' the other adjustment constants. $\mathcal{B}_{COAREG}$ further depends
340 on the choice of the W parameterization. Its original value of 1.8 was tuned to the SO
341 GasEx data using the Monahan and O'Muircheartaigh (1980) W parameterization which
342 was shown to highly over estimate W at high wind speeds (Brumer et al., 2017b). Based
343 on the HiWinGS data set, Blomquist et al. (2017) updated $\mathcal{B}_{COAREG}$ to equal 3.8 which

is close to the value found in the present study. Although the same parameterization is at the base of the bubble-mediated transfer in the present framework and in COAREG, $\mathcal{B}$ and $\mathcal{B}_{COAREG}$ are not directly comparable as they depend on the measure of the bubble air volume flux (F_a) used and on χ (Eq. 7). The bubble air volume flux estimated here from the breaking crest length distribution is about twice as large as that computed in COAREG using 2450 W.

Values of these empirical factors are not independent and reflect the uncertainties in the breaking crest length derived statistics. The choice of U_b and B will impact $\mathcal{B}$ and $\mathcal{C}$ which further account for the fact that we are dealing with estimates of the integrated flux of bubble plumes without resolving variations in the bubble size distributions and the flux and lifetime of individual bubbles. The empirical constants $\mathcal{A}$ and $\mathcal{B}$ could be interpreted as efficiencies of the turbulent driven and bubble mediated transfer, respectively. $\mathcal{C}$ encompasses the fact that full equilibration depends on the the limited volume of water between bubbles which is linked to the void fraction. A constant $\mathcal{C}$ does not allow for any variation (sea-state dependent or other) of the void fraction. A form of K_b including a breaking crest length dependent void fraction is derived in SI. It contains more unknowns and results in more scatter.

4.2 Remaining unknowns and limitations

Although the assumed functional form follows the typical approach used in other process based models, it may not be entirely correct. Indeed, it is not the gas transfer velocities that should be combined linearly, but rather the bubble- and turbulence-mediated fluxes ($F_g = F_\varepsilon + F_b$). The partial pressure of a gas within a bubble is higher than that in the atmosphere due to the pressure caused by the surface tension of the bubble skin, which can be estimated from the Young-Laplace equation and hydrostatic pressure of the surrounding water. Estimation of this excess pressure a bubble requires knowledge of the bubble size distribution as a function of depth and time.

The formulations of the bubble air volume flux contain several unknowns other than the bubble plume depth discussed above. The first unknown is the bubble cloud constant B which was set to 0.1 in accordance to Deike et al. (2016, 2017). B was determined from laboratory data from Duncan (1981), Lamarre and Melville (1991) and Deane and Stokes (2002) for time averaged volumes of air entrained $\bar{V}$ by a single breaking wave ranging

several orders of magnitude ($10^{-7} < \bar{V} < 10^{-1}$ m^3). The relationship however does not hold for $\bar{V} < 10^{-5}$ m^3 and it is unclear how these scale for open ocean conditions. The other unknown is the dissipation-weighted vertical mean bubble plume rise velocity (U_b). A constant U_b of 10 cm s^{-1} was used, corresponding to the rise terminal rise velocity of clean bubble of radius of 450 μm according to Woolf and Thorpe (1991). It is of the same order of magnitude as the rise velocity measured by Asher et al. (1997) in a sea-water tank which averaged around 8 cm s^{-1} within the first 6 seconds. Deike et al. (2017) proposed the following parameterization for U_b:

$$U_b \sim h/\tau_{br} \tag{22}$$

where h is the height of the wave at the time of breaking. While h is not measured directly it may be approximated as the significant height of the wind-sea ($H_{s_{ws}}$). The proportionality factor has however yet to be established. Since $H_{s_{ws}}$ ranges from ∼0.1 to 8 m and τ_{br} is on the order of 1-10 s, a proportionality coefficient equal to 1, as suggested by Deike et al. (2017), would lead to rise velocities ranging from a couple of centimeters a second to over a meter a second which is clearly too high.

Choosing a scale dependent U_b such as given by Eq. (22) would make F_a a function of the 5$^{\text{th}}$ moment of $\Lambda(c)$ (c.f. Eq. 17). To date there is not enough independent evidence or a sound physical argument to rule on the validity of one formulation over the other. This is also true with regards to the approach taken here versus that of Deike and Melville (2018) whose F_a is a function of the 3$^{\text{rd}}$ moment of $\Lambda(c)$. The fundamental difference is that they take a scale dependent $b(c)$ rather than b_{eff} based on the assumption that c_{br} may be related to a wavenumber through the deep water dispersion relation (Romero et al., 2012). Validity of this transformation has however been challenged (Zappa et al., 2016; Banner et al., 2014).

Finally, throughout this framework, a Schmidt number exponent of $\frac{1}{2}$ is used (Eqs. (4), (5)) which is in accordance with open ocean scaling. The exponent was suggested to vary between $\frac{1}{2}$ for wavy, surfactant free conditions to $\frac{2}{3}$ for flat, film covered surfaces. The exponent may therefor need adjustment for coastal applications and other surfactant-influenced surface conditions. The impact of surface-active material on the framework's coefficients ($\mathcal{A}$, $\mathcal{B}$, $\mathcal{C}$) remains unknown.

5 Conclusions

A novel framework to model the gas transfer velocity of sparingly soluble gases under breaking wave conditions in the open ocean is presented herein. It allows for estimations based on the breaking crest length distributions and sea state. As such it is applicable to purely remotely sensed data. Tuned to measurements from the HiWinGS field campaign it performs comparably to the COAREG algorithms. Higher noise in breaking length derived statistics compared to whitecap and friction velocity estimates accounts for relatively poorer results of the breaking crest length dependent model compared to COAREG. Unknowns remain in the formulation of the bubble-mediated transfer as is the case with other physically based models put forward in the literature. Measurements of bubble plumes in the ocean are necessary for further improvement.

Acknowledgments

The authors acknowledge Dr. Gemmrich who provided the original Matlab code to breaking crest length tracking that was adapted to the HiWinGS data. The analysis for the HiWinGS project was funded by the National Science Foundation (Grants OCE-1537890). Data used in the analysis described here have been made available through NOAA's Physical Sciences Laboratory repository (https://psl.noaa.gov/psd3/cruises/). S. E. Brumer was supported by a postdoctoral grant of the Centre National d'Études Spatiales (CNES).

References

Agrawal, Y. C., Terray, E. A., Donelan, M. A., Hwang, P. A., Williams III, A., Drennan, W. M., Kahma, K. K., and Kitaigorodskii, S. A. (1992). Enhanced dissipation of kinetic energy beneath surface waves. *Nature*, 359:219–20.

Asher, W. E., Karle, L. M., and Higgins, B. J. (1997). On the differences between bubble-mediated air-water gas transfer in freshwater and seawater. *Journal of Marine Research*, 55:813–845.

Asher, W. E., Karle, L. M., Higgins, B. J., Farley, P. J., Monahan, E. C., and Leifer, I. S. (1996). The influence of bubble plumes on air-seawater gas transfer velocities. *Journal Of Geophysical Research*, 101(C5):12027–12041.

Asher, W. E. and Wanninkhof, R. (1998). The effect of bubble-mediated gas transfer on purposeful dual-gaseous tracer experiments. *Journal of Geophysical Research*, 103(C5):10555–60.

Atmane, M. A., Asher, W. E., and Jessup, A. T. (2004). On the use of the active infrared technique to infer heat and gas transfer velocities at the air-water free surface. *Journal of Geophysical Research*, 109:C08S14.

Banerjee, S., Lakehal, D., and Fulgosi, M. (2004). Surface divergence models for scalar exchange between turbulent streams. *International Journal of Multiphase Flow*, 30(7):963–977. A Collection of Papers in Honor of Professor G. Yadigaroglu on the Occasion of his 65th Birthday.

Banerjee, S. and MacIntyre, S. (2004). The air-water interface: Turbulence and scalar exchange. *Advances in coastal and ocean engineering*, 9:181.

Banerjee, S., Scott, D. S., and Rhodes, E. (1968). Mass transfer to falling wavy liquid films in turbulent flow. *Industrial and Engineering Chemistry Fundamentals*, 7(1):22–27.

Banner, M. L. and Peirson, W. L. (2007). Wave breaking onset and strength for two-dimensional deep-water wave groups. *Journal of Fluid Mechanics*, 585:93–115.

Banner, M. L., Zappa, C. J., and Gemmrich, J. (2014). A note on phillips' spectral framework for ocean whitecaps. *Journal of Physical Oceanography*, 44(7):1727–1734.

Batchelor, G. K. (1959). Small-scale variation of convected quantities like temperature in turbulent fluid. part 1. general discussion and the case of small conductivity. *Journal of Fluid Mechanics*, 5:113–133.

Blomquist, B. W., Brumer, S. E., Fairall, C. W., Huebert, B. J., Zappa, C. J., Brooks, I. M., Yang, M., Bariteau, L., Prytherch, J., Hare, J. E., Czerski, H., Matei, A., and Pascal, R. W. (2017). Wind speed and sea state dependencies of air-sea gas transfer: Results from the high wind speed gas exchange study (HiWinGS). *Journal of Geophysical Research: Oceans*, 122(10):8034–8062.

Brumer, S. E., Zappa, C. J., Blomquist, B. W., Fairall, C. W., Cifuentes-Lorenzen, A., Edson, J. B., Brooks, I. M., and Huebert, B. J. (2017a). Wave-related reynolds number parameterizations of CO_2 and DMS transfer velocities. *Geophysical Research Letters*, 44(19):9865–9875. 2017GL074979.

Brumer, S. E., Zappa, C. J., Brooks, I. M., Tamura, H., Brown, S. M., Blomquist, B., Fairall, C. W., and Cifuentes-Lorenzen, A. (2017b). Whitecap coverage dependence on wind and wave statistics as observed during so gasex and hiwings. *Journal of Physical Oceanography*.

Cipriano, R. and Blanchard, D. (1981). Bubble and aerosol spectra produced by a laboratory "breaking wave". *Journal of Geophysical Research*, 86:8085–8092.

Danckwerts, P. V. (1951). Significance of liquid-film coefficients in gas absorption. *Industrial and Engineering Chemistry*, 43(6):1460–1467.

Deane, G. B. and Stokes, M. D. (2002). Scale dependence of bubble creation mechanisms in breaking waves. *Nature*, 418(6900):839–844.

Deike, L. (2022). Mass transfer at the ocean?atmosphere interface: The role of wave breaking, droplets, and bubbles. *Annual Review of Fluid Mechanics*, 54(1):null.

Deike, L., Lenain, L., and Melville, W. K. (2017). Air entrainment by breaking waves. *Geophysical Research Letters*, 44(8):3779–3787. 2017GL072883.

Deike, L. and Melville, W. K. (2018). Gas transfer by breaking waves. *Geophysical Research Letters*, 45(19):10,482–10,492.

Deike, L., Melville, W. K., and Popinet, S. (2016). Air entrainment and bubble statistics in breaking waves. *Journal of Fluid Mechanics*, 801:91–129.

Drazen, D. A., Melville, W. K., and Lenain, L. (2008). Inertial scaling of dissipation in unsteady breaking waves. *Journal of Fluid Mechanics*, 611:307–332.

Duncan, J. H. (1981). An experimental investigation of breaking waves produced by a towed hydrofoil. *Proceedings of the Royal Society of London, Series A*, 377(1770):331–48.

Duncan, J. H. (1983). The breaking and non-breaking wave resistance of a two-dimensional hydrofoil. *Journal of Fluid Mechanics*, 126:507–20.

Esters, L., Landwehr, S., Sutherland, G., Bell, T. G., Christensen, K. H., Saltzman, E. S., Miller, S. D., and Ward, B. (2017). Parameterizing air-sea gas transfer velocity with dissipation. *Journal of Geophysical Research: Oceans*, 122(4):3041–3056.

Fairall, C. W., Yang, M., Bariteau, L., Edson, J. B., Helmig, D., McGillis, W., Pezoa, S., Hare, J. E., Huebert, B., and Blomquist, B. (2011). Implementation of the coupled ocean-atmosphere response experiment flux algorithm with CO_2, dimethyl sulfide, and O_3. *Journal of Geophysical Research*, 116(C00F09):C00F09.

Gemmrich, J. R. (2010). Strong turbulence in the wave crest region. *J. Phys. Oceanogr.*, 40:583–595.

Gemmrich, J. R., Banner, M. L., and Garrett, C. (2008). Spectrally resolved energy dissipation and momentum flux of breaking waves. *J. Phys. Oceanogr.*, 38:1296–

1312.

Gemmrich, J. R., Zappa, C. J., Banner, M. L., and Morison, R. P. (2013). Wave breaking in developing and mature seas. *Journal of Geophysical Research - Oceans*, 118:4542–4552.

Goddijn-Murphy, L., Woolf, D. K., Callaghan, A. H., Nightingale, P. D., and Shutler, J. D. (2016). A reconciliation of empirical and mechanistic models of the air-sea gas transfer velocity. *Journal of Geophysical Research: Oceans*, 121(1):818–835.

Harriott, P. (1962). A random eddy modification of the penetration theory. *Chemical Engineering Science*, 17:149–154.

Higbie, R. (1935). The rate of absorption of a pure gas into a still liquid during short periods of exposure. *Trans. A.I.C.E.*, 31:365–389.

Ho, D., Sabine, C. L., Hebert, D., Ullman, D. S., Wanninkhof, R., Hamme, R. C., Strutton, P. G., Hales, B., Edson, J. B., and Hargreaves, B. R. (2011). Southern ocean gas exchange experiment: Setting the stage. *Journal of Geophysical Research - Oceans*, 116(C4):C00F08.

Keeling, R. F. (1993). On the role of large bubbles in air-sea gas exchange and supersaturation in the ocean. *J. Mar. Res.*, 51:237–271.

Kitaigorodskii, S. A. (1984). On the fluid dynamical theory of turbulent gas transfer across an air-sea interface in the presence of breaking wind-waves. *Journal of Physical Oceanography*, 14(5):960–972.

Kleiss, J. M. (2009). *Airborne observations of the kinematics and statistics of breaking waves*. PhD thesis, Scripps Institution of Oceanography-University of California.

Kleiss, J. M. and Melville, W. K. (2010). Observations of wave breaking kinematics in fetchlimited seas. *J. Phys. Oceanogr.*, 40:2575–2604.

Komori, S., Nagaosa, R., and Murakami, Y. (1993). Turbulence structure and heat and mass transfer mechanism at a gas-liquid interface in a wind-wave tunnel. *Applied Scientific Research*, 51:423–427.

Lamarre, E. and Melville, W. K. (1991). Air entrainment and dissipation in breaking waves. *Nature*, 351(6326):469–72.

Lamont, J. C. and Scott, D. S. (1970). An eddy cell model of mass transfer into the surface of a turbulent liquid. *A.I.Ch.E. J.*, 16:512–519.

Liang, J.-H., Deutsch, C., McWilliams, J. C., Baschek, B., Sullivan, P. P., and Chiba, D. (2013). Parameterizing bubble-mediated air-sea gas exchange and its effect on ocean ventilation. *Global Biogeochemical Cycles*, 27(3):894–905.

McCready, M. J., Vassiliadou, E., and Hanratty, T. J. (1986). Computer simulation of turbulent mass transfer at a mobile interface. *AIChE Journal*, 32(7):1108–1115.

McKenna, S. P. and McGillis, W. R. (2004). Observations of flow repeatability and secondary circulation in an oscillating grid-stirred tank. *Physics of Fluids*, 16(9):3499–3502.

Melville, W. K. (1994). Energy dissipation by breaking waves. *Journal of Physical Oceanography*, 24(10):2041–9.

Merlivat, L., Memery, L., and Boutin, J. (1993). Gas exchange at the air-sea interface: present status. case of CO_2. In *The Fourth International Conference on CO_2 in the OceansInst. Natl. des Sci. de l'Univers., Cent. Natl. de la Rech. Sci. Carqueiranne, FranceSept*, pages 13–17.

Monahan, E. C. and O'Muircheartaigh, I. (1980). Optimal power-law description of oceanic whitecap coverage dependence on wind speed. *Journal of Physical Oceanography*, 10(12):2064–2099.

Phillips, O. M. (1985). Spectral and statistical properties of the equilibrium range in wind-generated gravity waves. *Journal of Fluid Mechanics*, 156:505–31.

Phillips, O. M., Posner, F. L., and Hansen, J. P. (2001). High range resolution radar measurements of the speed distribution of breaking events in wind-generated ocean waves: Surface impulse and wave energy dissipation rates. *Journal of Physical Oceanography*, 31(2):450–460.

Rapp, R. J. and Melville, W. K. (1990). Laboratory measurements of deep-water breaking waves. *Philosophical Transactions of the Royal Society of London A*, 331(1622):735–800.

Romero, L., Melville, W. K., and Kleiss, J. (2012). Spectral energy dissipation due to surface-wave breaking. *J. Phys. Oceanogr.*, pages 1421–1444.

Schwendeman, M., Thomson, J., and Gemmrich, J. R. (2014). Wave breaking and dissipation in a young wind sea. *Journal of Physical Oceanography*, 44(1):104–127.

Shuiqing, L. and Dongliang, Z. (2016). Gas transfer velocity in the presence of wave breaking. *Tellus B: Chemical and Physical Meteorology*, 68(1):27034.

Sutherland, P. and Melville, W. K. (2013). Field measurements and scaling of ocean surface wave-breaking statistics. *Geophysical Research Letters*, 40:3074–3079.

Sutherland, P. and Melville, W. K. (2015). Field measurements of surface and near-surface turbulence in the presence of breaking waves. *Journal of Physical Oceanography*, 45(4):943–965.

Terray, E. A., Donelan, M. A., Agrawal, Y. C., Drennan, W. M., Kahma, K. K., A. J. Williams, I., Hwang, P. A., and Kitaigorodskii, S. A. (1996). Estimates of kinetic energy dissipation under surface waves. *Journal of Physical Oceanography*, 26(5):792–807.

Thomson, J., Gemmrich, J. R., and Jessup, A. T. (2009). Energy dissipation and the spectral distribution of whitecaps. *Geophys. Res Lett.*, 35:L11601.

Thorpe, S. A. and Hall, A. J. (1983). The characteristics of breaking waves, bubble clouds, and near-surface currents observed using side-scan sonar. *Continental Shelf Research*, 1(4):353–384.

Tokoro, T., Kayanne, H., Watanabe, A., Nadaoka, K., Tamura, H., Nozaki, K., Kato, K., and Negishi, A. (2008). High gas-transfer velocity in coastal regions with high energy-dissipation rates. *Journal of Geophysical Research: Oceans*, 113(C11):C11006.

Turney, D. E., Smith, W. C., and Banerjee, S. (2005). A measure of the near-surface fluid motions that predicts air-water gas transfer in a wide range of conditions. *Geophysical Research Letters*, 32:L04607.

Vachon, D., Prairie, Y. T., and Cole, J. J. (2010). The relationship between near-surface turbulence and gas transfer velocity in freshwater systems and its implications for floating chamber measurements of gas exchange. *Limnology and Oceanography*, 55(4):1723–1732.

Wanninkhof, R. (1992). Relationship between wind speed and gas exchange over the ocean. *Journal of Geophysical Research*, 97(C5):7373–7382.

Woolf, D. K. (1993). Bubbles and the air-sea transfer velocity of gases. *Atmos. Ocean*, 31:517–540.

Woolf, D. K. (1997). *Bubbles and their role in air-sea gas exchange*, pages 173–206. Cambridge Univ Press, Cambridge, UK.

Woolf, D. K., Leifer, I. S., Nightingale, P. D., Rhee, T. S., Bowyer, P., Caulliez, G., de Leeuw, G., Larsen, S. E., Liddicoat, M., Baker, J., and Andreae, M. O.

(2007). Modelling of bubble-mediated gas transfer: Fundamental principles and a laboratory test. *Journal of Marine Systems*, 66(1-4):71–91.

Woolf, D. K. and Thorpe, S. A. (1991). Bubbles and the air-sea exchange of gases in near saturation conditions. *J. Mar. Res.*, 49:435–466.

Yang, M., Blomquist, B., and Nightingale, P. D. (2014). Air-sea exchange of methanol and acetone during hiwings: Estimation of air phase, water phase gas transfer velocities. *Journal of Geophysical Research: Oceans*, 119(10):7308–7323.

Zappa, C. J., Banner, M. L., Gemmrich, J. R., Schultz, H., Morison, R. P., LeBel, D. A., and Dickey, T. (2012). An overview of sea state conditions and air-sea fluxes during radyo. *Journal of Geophysical Research - Oceans*, 117:C00H19.

Zappa, C. J., Banner, M. L., Morison, R. P., and Brumer, S. E. (2016). On the variation of the effective breaking strength in oceanic sea states. *Journal of Physical Oceanography*, 46(7):2049–2061.

Zappa, C. J., Ho, D. T., McGillis, W. R., Banner, M. L., Dacey, J. W. H., Bliven, L. F., Ma, B., and Nystuen, J. (2009). Rain-induced turbulence and air-sea gas transfer. *Journal Of Geophysical Research Oceans*, 114:C07009.

Zappa, C. J., McGillis, W. R., Raymond, P. A., Edson, J. B., Hintsa, E. J., Zemmelink, H. J., Dacey, J. W. H., and Ho, D. T. (2007). Environmental turbulent mixing controls on the air-water gas exchange in marine and aquatic systems. *Geophysical Research Letters*, 34(L10601):doi:10.1029/ 2006GL028790.